Journal of Applied Polymer Science

Polypropylene-based composites containing sorbitol-based nucleating agent and siloxane-silsesquioxane resin

Monika Dobrzyńska-Mizera,[1] Michał Dutkiewicz,[2] Tomasz Sterzyński,[1] Maria Laura Di Lorenzo[3]
[1]Poznan University of Technology, Institute of Materials Technology, Polymer Division, Piotrowo, 3, Poznan 61-138, Poland
[2]Centre for Advanced Technologies, Adam Mickiewicz University, Umultowska, 89 C, Poznan 61-614, Poland
[3]Consiglio Nazionale Delle Ricerche, Istituto per I Polimeri, Compositi E Biomateriali, c/o Comprensorio Olivetti, via Campi Flegrei, 34, Pozzuoli, NA 80078, Italy
Correspondence to: M. Dobrzyńska-Mizera (E-mail: monika.dobrzynska-mizera@put.poznan.pl)

ABSTRACT: Composites based on isotactic polypropylene (iPP) modified with a sorbitol derivative (NX8000) and siloxane-silsesquioxane resin containing reactive phenyl groups (SiOPh) were prepared by melt extrusion. These iPP-based formulations were investigated to evaluate the influence of such additives on the crystallization behavior and morphology, as well as on thermal and mechanical properties. The addition of sorbitol fastens crystallization kinetics of iPP and leads to higher transparency of iPP films. Upon the incorporation of siloxane-silsesquioxane resin, no further effect on iPP crystallization kinetics is evidenced by calorimetry, optical microscopy, and X-ray diffraction analysis. Transparency of iPP-based composites is improved upon the addition of sorbitol, but decreased when SiOPh is added to the formulation. The composites are also stiffer, compared to neat polypropylene with a decreased elongation at break and increased Young's modulus values, with increasing amounts of fillers. The effect of the siloxane-silsesquioxane resin on properties of iPP/NX8000/SiOPh composites was explained taking into account compatibility of the components and morphology of the composites. © 2016 Wiley Periodicals, Inc. J. Appl. Polym. Sci. **2016**, *133*, 43476.

KEYWORDS: composites; crystallization; differential scanning calorimetry; morphology; polyolefins

Received 3 November 2015; accepted 23 January 2016
DOI: 10.1002/app.43476

INTRODUCTION

Isotactic polypropylene (iPP) is a semicrystalline and polymorphic thermoplastic with a maximum degree of crystallinity of 60–70%. iPP crystals of different structures and morphologies can be generated by variation of the crystallization conditions and/or by introducing nucleating agents into the polymeric matrix. As a result, iPP can develop various crystal modifications called α-, β-, γ-, δ- (in the presence of comonomers), and ε-structures, as well as a conformationally disordered mesophase.[1–5] The α-structure is technically important since it ensures to iPP better transparency as well as higher modulus and tensile strength, compared to the other crystal modifications.[6]

The most extensively used nucleating agents, which contribute to α-structure formation, are sorbitol derivatives, because of their high efficiency. Although the cost of sorbitol derivatives is quite high, their effect on optical properties is unique. Thus, they are commonly used as clarifiers and no cheaper additives, able to similarly improve iPP transparency, have been developed yet. The addition of sorbitol derivatives also results in increased crystallization temperature and decreased spherulite size.[7] Moreover, sorbitol derivatives are soluble in molten iPP, which allows easy and efficient dispersion during processing. As was recently demonstrated,[8,9] upon cooling from the melt, the sorbitols mixed with polypropylene undergo phase separation, with formation of a percolated network of fibrils which hosts a large number of nucleation sites for growth of iPP spherulites. This phenomenon is crucial from the application point of view, because an anticipated onset of nucleation leads to faster crystallization, which allows to shorten the cycle time and reduce the production cost, i.e., may be an advantage in case of injection molding process. Conversely, a too high crystallization rate may be a drawback for extrusion of products such as films or fibers, since creation of highly ordered and oriented chain segments occurs prior to crystallization process.[10] As a consequence, a too fast crystallization may limit production of highly oriented goods.

In recent years, many research efforts have been directed towards incorporation of organic–inorganic hybrid materials into iPP.[11–14] Such materials have organic components bonded to a siloxane or silica backbone and are variously referred to as organically modified silicas, ormosils, or silsesquioxanes (POSS). This class of

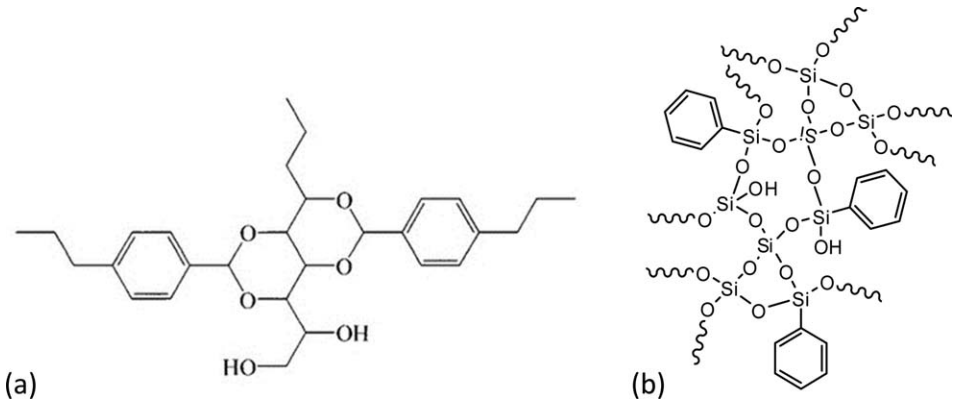

Figure 1. Chemical structures of (a) NX8000 and (b) SiOPh.

hybrids owes unique possibilities to combine the properties of the organic moieties with those of the siloxane or silica matrix. Moreover, the presence of organic groups increases hydrophobicity of the particle surface, resulting in a potential improvement in compatibility between filler and host polymer.[15] Despite all these advantages, it was shown that these organic–inorganic hybrids are poorly compatible with iPP.[16–18] An alternative approach consists of combining commercially used nucleating agents with organic–inorganic materials.[19–22] Roy *et al.*[23] reported that the molecules of silanol silsesquioxanes and a sorbitol derivative, namely di(benzylidene)sorbitol, are capable of forming several complex molecular adducts, due to noncovalent interactions, i.e., hydrogen bonding. Formation of the molecular complex prevents fibrillation of the sorbitol derivatives, which also reduces their nucleation efficiency, and in turn allows to tailor the crystallization kinetics of iPP by modulating formulation of the fillers.[24] Unfortunately, the high cost of commercial POSS has limited its use so far, and there is still a need to seek for lower cost modifiers.

As an effort to find lower cost additives able to tailor the crystallization kinetics of iPP containing sorbitol derivatives, a number of novel phenyl siloxane-silsesquioxane resins were synthesized in our laboratory. They contain silanol groups which are expected to interact with the functional groups of sorbitol,[24] as well as side alkyl groups that may promote blending with polyolefins.[25] Such resins were tested as fillers for iPP, together with commercial sorbitols as nucleating agents.

In this article, the influence of one such resin on crystallization kinetics of iPP containing a commercial clarifying agent, namely, 1,2,3-tridesoxy-4,6:5,7-bis-*O*-[(4-propylphenyl)methylene]nonitol sorbitol, (NX8000) is discussed. In a forthcoming article, the influence of a different sorbitol derivative and siloxane-silsesquioxane resin on iPP properties will be detailed. The aim is to investigate the influence of such additives on the crystallization behavior and morphology, as well as on thermal and mechanical properties of iPP nucleated with the modified sorbitol, as a function of the molecular characteristics of both the sorbitol derivative and phenyl siloxane-silsesquioxane resin. The goal is to develop an iPP-based formulation whose crystallization kinetics is tailored for extrusion processing, to optimize material properties taking into account also production costs.

EXPERIMENTAL

Materials

A commercial iPP Midilena III PPF401, with MFR = 3 g 10 min^{-1} (230 °C, 2.16 kg) from Rompetrol Petrochemicals S.R.L. (Romania) was used in our experiments. The selected iPP grade is characterized by a low modification level, i.e., there are no plasticizers, colored masterbatches or nucleating agents added.

The sorbitol derivative added to iPP is 1,2,3-tridesoxy-4,6:5,7-bis-*O*-[(4-propylphenyl)methylene]nonitol sorbitol, Millad NX8000 (NX8000), which was kindly provided by Milliken Chemical Company (Belgium). Previous investigations revealed that 0.25 wt % is an amount of NX8000 adequate to promote crystal nucleation in iPP.[9] Siloxane-silsesquioxane resin modified with phenyl groups of general formula [PhSiO1.5]n, abbreviated SiOPh, which acts as a modifier for the nucleating agent, was synthesized in our laboratory as detailed below. The thermal stability of all materials was determined using thermogravimetry (TGA), which proved that all the components do not undergo thermal degradation at the used processing temperatures of iPP. The chemical formulas of NX8000 and SiOPh are presented in Figure 1.

Preparation of SiOPh

The synthesis was conducted using two-step acid-base co-condensation of tetraethoxysilane and phenyltriethoxysilane mixture in 2:1 molar ratio, following the procedure detailed in.[26,27] Tetraethoxysilane, phenyltriethoxysilane and tetrahydrofuran (THF), in an amount of twice the volume of the silanes used, were placed in a flask equipped with a mechanical stirrer. The solution was stirred for 30 min to homogenize the ingredients. Then, an aqueous solution of hydrochloric acid in water (1.5 mL of 35.5% HCl in 100 mL of water) was added into the solution of silanes in THF in order to acidify the reaction medium. Once the acid was added, the reaction mixture became turbid. After about 15 min, turbidity disappeared and a rise in temperature occurred. Stirring was maintained for 60 min to cool down the mixture to room temperature. Next, aqueous ammonia solution was added dropwise to basify the reaction medium (3.5 mL of 25% aqueous ammonia in 200 mL of water). Upon the addition of alkali, the mixture underwent turbidity again (formation of the product). After the addition was completed, an intensive stirring was maintained for additional 60 min. Afterward, the mixture was filtered, washed twice with 100 ml of water and dried for 24 h at 120 °C.

Table I. Designations and Mass Concentrations of Obtained Samples

	Mass concentration (%)		
Designation	iPP	NX8000	SiOPh
iPP	100	0	0
iPP+NX8000	99.75	0.25	0
iPP+NX+0.1SiOPh	99.65	0.25	0.1
iPP+NX+0.5SiOPh	99.25	0.25	0.5
iPP+NX+1SiOPh	98.75	0.25	1
iPP+NX+3SiOPh	96.75	0.25	3

Sample Preparation

Polypropylene pellets were milled into powder with a Tria high-speed grinder. The polymer was mixed with the sorbitol derivative and SiOPh in the rotary mixer Retsch GM 200 for 3 min at a rotation speed of 3000 rpm. Homogenization of the premixed materials with different SiOPh contents (0.1–3 wt %) and a fixed sorbitol concentration of 0.25 wt % was ensured by molten state extrusion with a Zamak corotating twin screw extruder operated at 190 °C and 70 rpm. The extruded rod was pelletized in a water bath. iPP/NX8000/SiOPh composites at various compositions were prepared, as summarized in Table I.

The composites were compression-molded with a Collin Hydraulic Laboratory Forming Press P 200 E at a temperature of 200 °C for 3 min, without any pressure applied, to allow complete melting. After this period, a load of about 10 MPa was applied for 3 min, and then the samples were cooled to room temperature in less than 3 min by means of cold water circulating in the plates of the press. iPP-based sheets with a thickness of 150 μm and 1.2 mm were obtained. The thin films were used for the study of crystallization kinetics, to optimize heat dissipation during the phase transition, whereas the thick films were used for the investigation of mechanical properties of the materials, to comply with ISO standards.

Methodology

Attenuated Total Reflectance (ATR). Infrared spectra were collected with a Bruker Tensor 27 spectrometer in attenuated total reflectance (ATR) mode using 16 scans. The spectra resolution was 2 cm^{-1}. Sample specimens were measured as obtained, without additional preparation steps. Mid IR pyroelectric detector RT-DLaTGS/KBr was used in the study.

Differential Scanning Calorimetry (DSC). The thermal properties of iPP and its composites with NX8000 and SiOPh were investigated using a Mettler-Toledo DSC 822 differential scanning calorimeter, equipped with a liquid-nitrogen accessory for fast cooling. The calorimeter was calibrated in temperature and energy using indium. Dry nitrogen was used as purge gas at a rate of 30 mL min^{-1}.

To set the structure for the analysis of crystallization kinetics, each sample was heated from 25 to 200 °C at a rate of 20 °C min^{-1}, melted at 200 °C for 10 min to erase previous thermal history, quickly cooled to 160 °C at 20 °C min^{-1} to limit as much as possible the exposure to high temperatures, then cooled to −60 °C at various rates, ranging from 0.5 to 4 °C min^{-1}. After completion of crystallization, the composites were heated again at 20 °C min^{-1} until complete melting.

Crystallization is an exothermic process, and the heat evolved during the phase transition may cause some local heating and thermal gradients within the sample. As a consequence, transitions can occur at temperatures that do not correspond to those detected by the instrumentation.[28,29] The thicker the sample, the more critical this problem is. In order to reduce these problems, sample mass was limited to 3.0 ± 0.2 mg, and cooling rates not exceeding 4 °C min^{-1} were used.

Polarized Optical Microscopy (POM). Spherulite growth rates were estimated by optical microscopy, using a Zeiss polarizing microscope equipped with a Linkam TMHS 600 hot stage. A small piece of compression-molded sample was squeezed between two microscope slides and then inserted in the hot stage. The thickness of the squeezed sample was lower than 10 μm. The radius of the growing crystals was monitored during solidification by taking photomicrographs at appropriate intervals of time, using a Scion Corporation CFW-1312C Digital Camera. Spherulite radii were measured with the software Image-Pro Plus 7.0.

The thermal treatments before isothermal and nonisothermal crystallizations were identical to those used in calorimetry. For nonisothermal crystallization, a self-nucleation procedure was used, to expand the temperature range of analysis. Each sample was heated from 25 to 200 °C at a rate of 20 °C min^{-1}, melted at 200 °C for 10 min to erase previous thermal history, cooled to 155 °C at 30 °C min^{-1}, and maintained at 155 °C until the appearance of the first crystals. Then, the temperature was raised to 160 °C by heating at 30 °C min^{-1}, equilibrated at 160 °C, then the samples were cooled at 0.5 °C min^{-1} until spherulite impingement.

Isothermal crystallization measurements at 150 and 153 °C were also conducted, to confirm reliability of the data gained using the nonisothermal procedure.

Haze. The optical behavior of the polymers was characterized by haze measurements carried out on the 150 μm compression molded films according to the PN-84/C-89100 standard[30] using a Haze Meter HM-150 produced by Murakami Color Research Laboratory (Japan).

Wide-Angle X-ray Diffraction (WAXD). WAXD measurements were performed on a Philips Analytical X-Ray, model PW 1830 diffractometer with Cu Kα radiation. The scanned 2θ range was from 2 to 45° with a scanning rate of 0.02°, time per step of 1 s and scanning speed of 0.02° s^{-1}. The samples used for WAXD analysis were in the form of compression molded sheets of 1.2 mm thickness. Characteristic peaks were assigned according to the literature.[31]

Scanning Electron Microscopy (SEM). Morphological analysis of cryogenically fractured iPP/NX8000/SiOPh composites was performed using a FEI Quanta 200 FEG environmental scanning electron microscope (SEM) (Eindhoven, The Netherlands) in low-vacuum mode, using a large field detector and an accelerating voltage of 10–20 kV. Before analysis, the samples were sputtered-coated with Au-Pd alloy using Baltech Med 020 Sputter Coater System and then mounted on aluminum stubs.

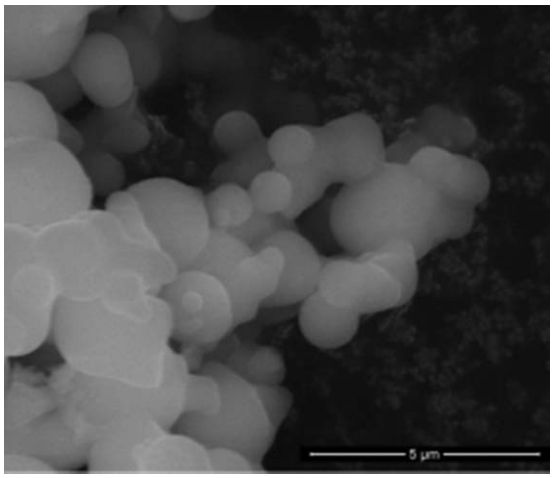

Figure 2. SEM micrograph showing morphology of SiOPh particles.

Static Tensile Tests. Mechanical properties of iPP-based compression-molded sheets were evaluated as per ISO 527[32] using Instron tensile tester, model 4505. Measurements of elastic modulus were conducted at a crosshead speed of 1 mm min^{-1}, to ensure deformation rate close to 1% of measuring section length per minute.[32] Whereas elongation at break was estimated at a speed of 50 mm min^{-1}, for a reasonable duration of the experiments, taking into account that tensile elongation at break mainly depends on material properties (inversely proportional to brittleness).[33,34]

RESULTS AND DISCUSSION

The preparation of siloxane-silsesquioxane resin has received considerable attention due to its complex structure, possible functionalization and low cost, in comparison to standard silsesquioxane molecules (POSS).[35] Hence, novel phenyl siloxane-silsesquioxane resin was synthesized and characterized in our laboratory. Morphology of the prepared particles was characterized by SEM. The SEM micrograph displayed in Figure 2 shows spherical SiOPh particles with a diameter of approximately 1 µm. It is also seen from the image that a good size distribution of the particles was achieved using the two-step acid-base condensation method detailed above.

Figure 3 presents the ATR spectrum of the SiOPh resin. All bands in the ATR spectrum confirm the structure of the obtained material. Broad bands at 3627 and 3390 cm^{-1} are attributed to the presence of silanol groups (respectively free OH and hydrogen-bonded ones). The band at 954cm^{-1} characteristic for Si−OH groups is also observed in the spectrum. The bands at 1631 and 571cm^{-1} indicates minor hydratation of the sample. The presence of phenyl groups is confirmed by the presence of stretching vibrations of C−H, C = C (3075, 3054, 1595 and 1431 cm^{-1}, respectively) as well as bending vibrations of =C−H bonds at 789, 738 and 697 cm^{-1}. A high intensity band, with two maxima at 1130 and 1049 cm^{-1}, results from stretching vibrations of Si−O−Si bands and is characteristic for silicon materials.[36] The maximum at 1049 cm^{-1} indicates the presence of smaller stretching Si−O−Si bands (<144°) and the one at 1130 cm^{-1} confirms those of about 144°. This split in oscillation region is related to the transverse and longitudinal valence oscillations of the atoms in siloxane bridge so the frequencies of the mentioned oscillations are distributed in separate regions from 1010 to 1140 cm^{-1} and 1190 to 1300 cm^{-1} in the range of θ from 120 to 180°.[37] This split can also be attributed to the simultaneous presence of Q and T units in the examined structure. The Q unit represents a silicon atom linked through siloxane bond to subsequent four silicon atoms forming a tetrahedron. Wherein, the T unit presents a silicon atom bonded to further three silicon atoms and one phenyl group.[38] The low intensity bands characteristic for stretching

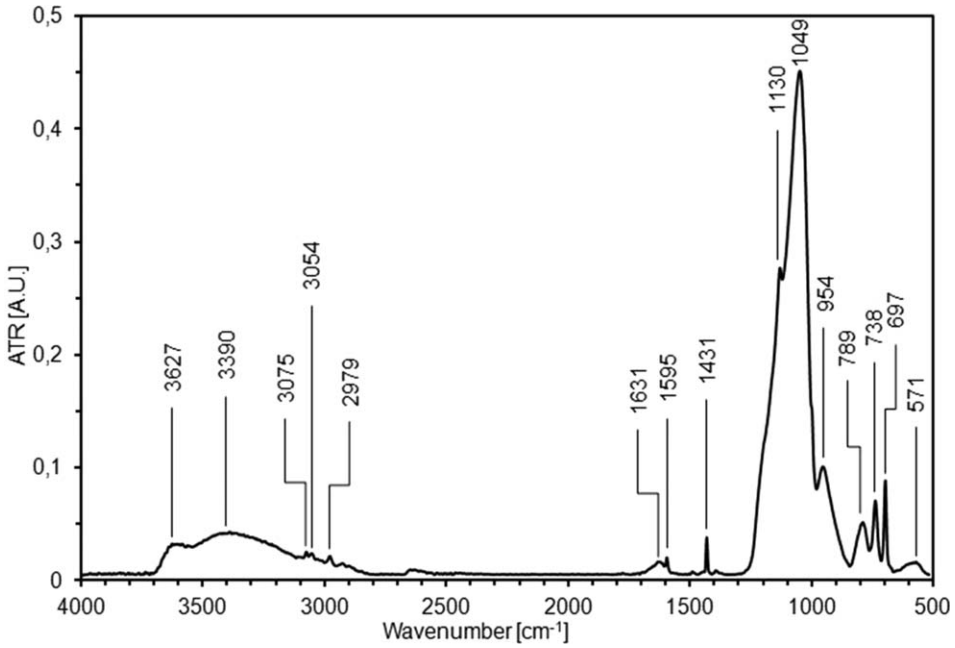

Figure 3. ATR spectrum of SiOPh resin.

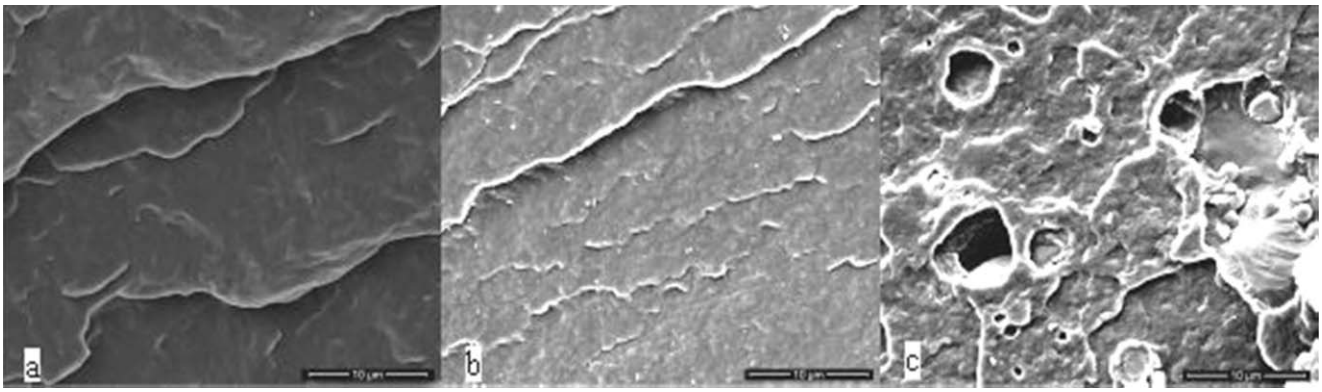

Figure 4. SEM micrographs for (a) iPP, (b) iPP + NX8000, and (c) iPP + NX + 3SiOPh.

vibrations of C−H bonds (sp^3 CH_3 and sp^2 CH_2 groups) at about 2979 and 2929 cm^{-1} appeared due to the presence of small amount of unreacted (not hydrolyzed) ethoxy groups. Obtaining such a structure, that is siloxane-silsesquioxane resin with POSS Q structures as network nodes with reactive phenyl groups in siloxane bridges between silsesquioxane (POSS) molecules, allows for replacement of expensive functionalized silsesquioxanes with this cheaper but still valuable chemical compound. Moreover, resin containing Q POSS units and reactive functional groups is, in principal, capable to interact with organic polymers and sorbitol derivatives, which will be studied in-depth and presented in this paper.

To gain information about the phase structure and morphology of the iPP composites containing sorbitol and resin, SEM analyses were performed. The results are presented in Figure 4. Figure 4(a) illustrates the cryogenically fractured surface of compression-molded plain iPP which appears quite smooth as expected. Morphology of iPP composite containing 0.25 wt % of NX8000 is exhibited in Figure 4(b). The fractured surface is quite smooth and similar to the one shown in Figure 4(a), with only small particles that adhere on iPP surface, possibly revealing the presence of sorbitol, although both the particle size and the very small amount added do not allow unequivocal interpretation. The fractured surface morphology changes drastically upon the addition of SiOPh, as illustrated in Figure 4(c), which presents the scanning electron micrograph of the sample containing 3 wt % of resin. A number of large voids of various dimensions are visible on the sample surface, possibly due to filler particles that are pulled out upon the cryogenically fracture process. At the same time, some nearly spherical particles, attached to the iPP matrix, also appear. The size of both the holes and particles indicates considerable filler agglomeration upon melt processing, since the average particle size of unprocessed SiOPh is ~1μm, as shown in Figure 2, much smaller that the spheres and voids seen in Figure 4(c).

Crystallization kinetics of the composites was studied by DSC and optical microscopy. Analyses were conducted upon cooling at various rates, ranging from 0.5 to 4 °C min^{-1}. The raw DSC curves are exampled in Figure 5(a) for the cooling rate of 4 °C min^{-1}. Plain iPP starts to crystallize at 129 °C, when cooled from the melt at 4 °C min^{-1}. Introduction of 0.25 wt % of sorbitol causes an anticipated increase of crystallization temperature onset (T_{onset}) to 137 °C, probing its efficiency as nucleating agent. Addition of 0.1–3 wt % of SiOPh does not induce significant variations in the crystallization profile of iPP nucleated with sorbitol, as all the DSC curves shown in Figure 5(a) practically overlap, within experimental error. The onset temperatures of the analyzed composites are plotted in Figure 5(b) as function of the cooling rate. The onset points were taken as the intersection of the baseline before the transition and the inflectional tangent of the crystallization exotherm,[29] and the peak temperature as the maximum of the exotherm. For every sample, with increasing cooling rate (χ), the crystallization curves shift to lower temperatures, as typical for polymer crystallization: at lower χ, there is more time to overcome the energy barriers for

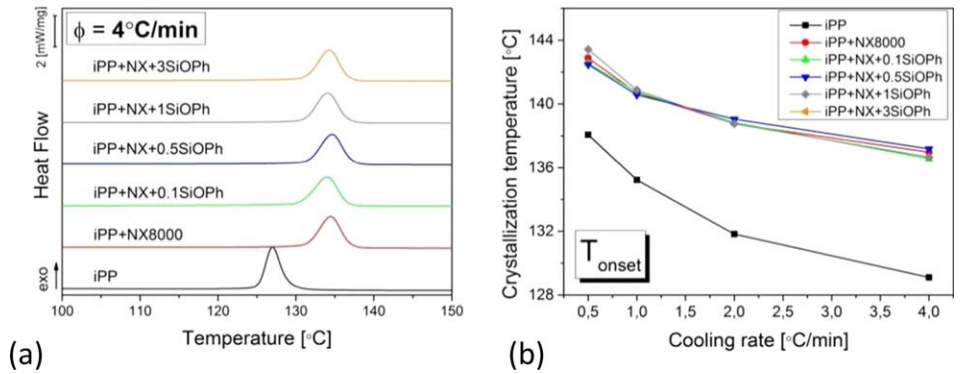

Figure 5. DSC crystallization curves and the onset crystallization temperature versus cooling rates. [Color figure can be viewed in the online issue, which is available at wileyonlinelibrary.com.]

Table II. Peak of Crystallization Temperature and Crystallinity Degrees for All Samples Cooled at Various Cooling Rates

	4 °C min^{-1}		2 °C min^{-1}		1 °C min^{-1}		0.5 °C min^{-1}	
	T_{peak} (°C)	X_C (%)	T_{peak} (°C)	X_C (%)	T_{peak} (°C)	X_C (%)	T_{peak} (°C)	X_C (%)
iPP	127.1	51	129.3	49	132.4	48	135.3	54
iPP+NX8000	134.4	50	136.4	52	138.2	50	139.3	53
iPP+NX+0.1SiOPh	134.1	51	136.6	51	138.4	51	140.3	53
iPP+NX+0.5SiOPh	134.6	51	136.5	50	138.2	48	139.6	52
iPP+NX+1SiOPh	134.1	50	136.2	49	137.7	51	140.0	51
iPP+NX+3SiOPh	134.3	51	136.1	51	138.0	53	139.3	52

nucleation, so that crystallization can start at higher temperatures, whereas at higher χ nuclei become active at lower temperatures.[39] In polymer samples containing added foreign particles, for a given cooling rate, the temperature at which crystallization starts is indicative of the effectiveness of the filler to promote heterogeneous nucleation.[40,41] The addition of 0.25 wt % of sorbitol induces crystallization to start at high temperatures compared to plain iPP, independently of the amount of SiOPh added to the formulation.

Sorbitol clarifiers are known to dissolve in molten iPP; they crystallize during cooling from the melt and can efficiently nucleate iPP spherulites when their concentration in polypropylene is above a threshold limit.[9,42] The latter is related to solubility and to the formation of a sorbitol network which arises from intermolecular hydrogen bonding and π–π interactions between the adjacent phenyl rings.[43–45] The used NX8000 concentration (0.25 wt %) is above this threshold concentration and iPP spherulites can start their growth on the fibrillar network formed upon crystallization of the sorbitol, as probed by the significantly increased onset temperature for crystallization. When the siloxane-silsesquioxane resin is added to the formulation, the nucleation efficiency of NX8000 is not affected. Both fillers have functional groups that may in principle interact upon melt mixing, by possible establishment of hydrogen bonds, influencing miscibility of the modified sorbitol with polypropylene and in turn, its efficiency as nucleating agent.[21] For all the analyzed compositions containing NX8000 and various amounts of SiOPh, the onset temperature is not affected by SiOPh, as shown in Figure 5(b). This indicates that limited or negligible interaction between NX8000 and SiOPh is established, and the modified sorbitol maintains its efficiency as nucleating agent for iPP, independently of resin content, at least for the analyzed composition range.

The main parameters derived by the non-isothermal crystallization experiments are summarized in Table II. The onset temperatures are plotted in Figure 5(b), hence are not repeated in Table II, which only displays the peak temperatures (T_p) and the crystallinity degree (X_c). The latter was calculated from the data obtained from the DSC plots gained during cooling at different cooling rates according to the following eq. (1):

$$X_C = \frac{\Delta H_M}{(1\text{-}\varphi)\Delta H_0} \times 100\% \quad (1)$$

where ΔH_M is the experimental heat of fusion, ΔH_0 is the enthalpy of fusion of the fully crystalline polymer, equal to 207.1 Jg^{-1},[46] and ϕ is the weight fraction of the modifiers. As reported in Table II, the crystal fraction developed upon cooling at rates up to 4 °C min^{-1} is $X_c = 50 \pm 2\%$, independently of composite composition. This indicates that addition of NX8000 only, or coupled with up to 3 wt % of SiOPh, does not affect crystallinity of polypropylene, under the chosen experimental conditions. It influences only crystallization kinetics of iPP, as the onset and peak points are shifted to higher temperatures due to enhanced nucleation of iPP spherulites.

Polarized optical microscopy was used to estimate the spherulite growth rate (G) of iPP and its composites with sorbitol and resin. To gain data in a wide temperature range, nonisothermal crystallization experiments were performed using a self-nucleation procedure.[47] Such method was chosen because of the high density of nucleation of the samples that contain sorbitol: at low temperatures, a high number of very small spherulites grow simultaneously, which hinders reliable analysis of the rate of their growth. Conversely, with self-nucleation and measurements upon continuous cooling, experiments are made when only a few iPP spherulites grow; they can reach relatively large dimensions, which permit reliable data analysis until impingement.

The measurements were conducted at a constant cooling rate so G can be estimated by taking the first derivative of the radius (r) vs. temperature (T) plot at each experimental point:

$$G = \frac{dr}{dt} = \frac{dr}{dT}\frac{dT}{dt} \quad (2)$$

where dr/dT is a measured point from the plot and dT/dt is the cooling rate.[48]

Figure 6 represents the spherulite growth rate vs. temperature plots for all studied samples. The data overlap, within experimental error, in all the analyzed temperature range, showing that the growth rate of iPP spherulites is not affected by addition of the fillers. During crystallization, the dispersed sorbitol and silicate particles must be rejected and/or occluded by the growing spherulites, which in principle can disturb spherulite growth: energy needs to be dissipated to reject, engulf, or deform the noncrystallizable additives, but likely such energy barrier is quite low and results in a negligible contribution to spherulite growth rate.

To determine a possible influence of the additives on crystal polymorphism of iPP, wide-angle X-ray diffractions (WAXD) analyses were performed. Figure 7 presents the WAXD patterns of three representative samples: pure iPP, iPP nucleated with

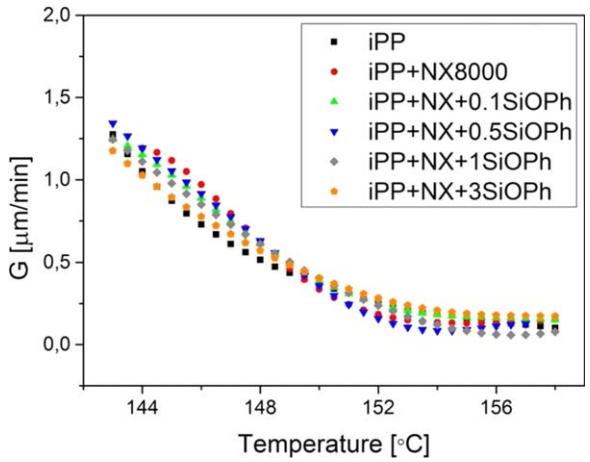

Figure 6. Spherulite growth rates of iPP and its composites measured upon cooling from the melt at 0.5 °C min^{-1}. [Color figure can be viewed in the online issue, which is available at wileyonlinelibrary.com.]

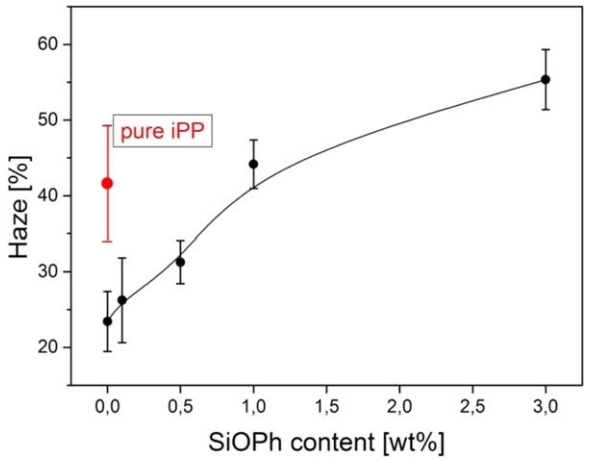

Figure 8. Dependence of haze on SiOPh concentration in iPP/NX8000 composite for compression-molded sheets. [Color figure can be viewed in the online issue, which is available at wileyonlinelibrary.com.]

NX8000, and iPP that contains both NX8000 and 3 wt % of SiOPh. The three samples display very similar WAXD profiles, with characteristic peaks at $2\theta = 14.1°$, 16.9°, 18.5°, 21.2°, and 21.8°, corresponding to (110), (040), (130), (111), and (041) α-phase, respectively. Moreover, no additional peaks at 16.2 and 19.8 corresponding to β and γ phases were noticed. This indicates the existence of only α structure in the samples. The crystal fraction measured by WAXD is also unaffected by addition of sorbitol and silicate, which confirms DSC results.

Overall, the addition of NX8000 favors nucleation of iPP, independently of the presence of SiOPh, and results in an anticipated onset of nucleation and faster crystallization kinetics. The latter depends only on the enhanced nucleation rate, being the rate of crystal growth unaffected by the presence of the additives. Moreover, the additives do not modify crystal polymorphism of iPP, at least for the analyzed compositions and crystallization conditions.

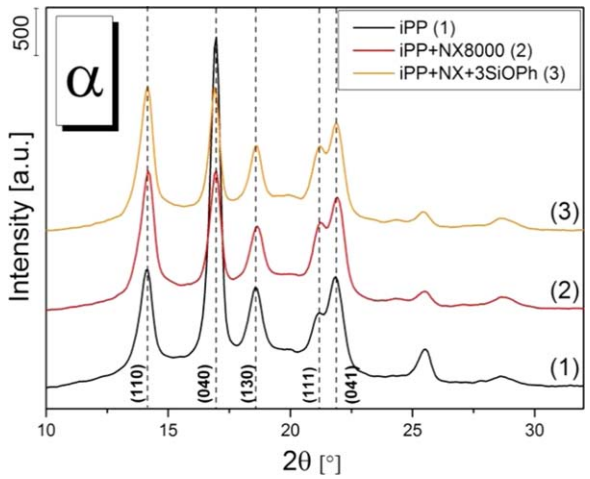

Figure 7. WAXD patterns of pure and modified polypropylene. [Color figure can be viewed in the online issue, which is available at wileyonlinelibrary.com.]

iPP crystals are made of chain folded fibrils or lamellae which are often large enough to interfere with visible light and this interference results in considerable haze that is often used for the characterization of the appearance of a plastic product. Haze is defined as the total flux of light scattered within the angular range between 2.5° and 90° and normalized to the total transmitted flux.[49]

The effect of nucleating agent and siloxane-silsesquioxane resin upon haze of iPP is presented in Figure 8. Introduction of sorbitol derivative results in a significant decrease in the haze value, which indicates that the nucleated sample was more transparent than pure iPP. However, the gradual addition of SiOPh results in worsening of matrix transparency, wherein the addition of 1 wt % and more results in haze values similar or higher than this for pure matrix. As shown by Horvath *et al.*,[50] crystallinity, spherulite size, lamella thickness, and probably also the interface area between the crystalline and amorphous phases may play a significant role in haze values. However, the principal parameter influencing haze is the spherulite size of the supermolecular structure formed during crystallization of polymer, wherein haze decreases with decreasing spherulite size. Addition of a nucleating agent results in a formation of fibrillar network hosting a large number of nucleation sites for growth of iPP spherulites. Hence, numerous smaller spherulites crystallize in nucleated polypropylene matrix resulting in improved clarity. As mentioned above, together with an increasing content of siloxane-silsesquioxane resin, a significant deterioration in transparency occurs. As evidenced in the SEM micrograph presented in Figure 4, the addition of SiOPh results in considerable filler agglomeration upon melt processing, thus agglomerates may interfere with visible light and result in a significant decrease in transparency.

Mechanical properties of the iPP/NX8000/SiOPh composites were determined using static tensile tests. Main parameters are summarized in Figure 9. Analysis of changes in the elastic modulus, reported in Figure 9(a), reveals a slight increase in this value for the nucleated sample in comparison to the pure one,

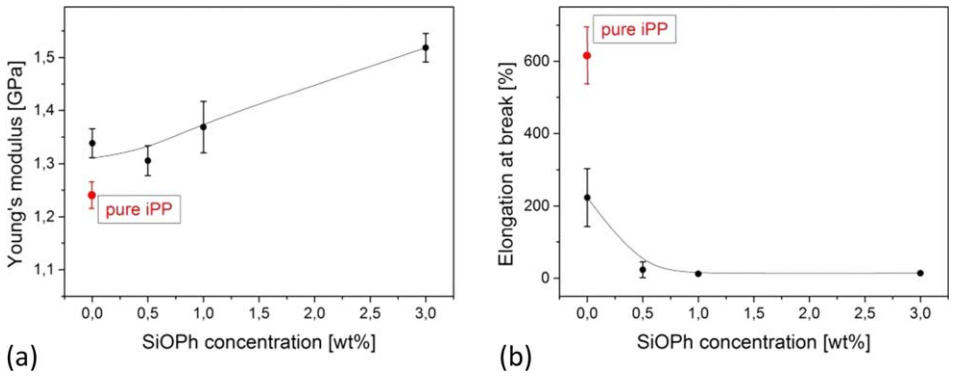

Figure 9. Mechanical properties of pure, nucleated and modified polypropylene matrix; (a) Young's modulus and (b) elongation at break (the lines were drawn to guide the eye). [Color figure can be viewed in the online issue, which is available at wileyonlinelibrary.com.]

from 1.25 to 1.5 GPa, and further rise to a maximum value of 1.56 GPa for the sample that contains the highest amount of modifiers. On the contrary, the addition of sorbitol derivative and an increasing amount of siloxane-silsesquioxane resin results in a continuous decrease in the elongation at break values, from 600% for pure polypropylene, down to 14% for the iPP+NX+3SiOPh sample. Moreover, a qualitative change in the stress-strain behavior was noted, since the samples that contain siloxane-silsesquioxane resin do not undergo yielding.

The mechanical properties of semicrystalline polymer composites depend markedly on composition and phase structure, as well as on crystal fraction, size and morphology. Some slightly increased lamellae thickness can be expected from the increased crystallization temperature in the nucleated samples, but no variation in crystal fraction or crystal modification was probed by DSC and WAXD analyses. Adhesion between the filler and the matrix largely affects the large strain properties such as the elongation at break, whereas the low-strain properties, like Young's modulus, are much less dependent on compatibilization of the components, being mostly additive.[51] As seen in Figure 4, the SiOPh particles are poorly bonded to the iPP matrix, thus behave as voids in the structure that facilitate the premature fracture upon deformation, which leads to a decreased elongation at break with increasing amounts of the filler.

CONCLUSIONS

This study details how a combination of modified sorbitol and siloxane-silsequixane resin influences properties of iPP-based composites. Addition of the sorbitol derivative to iPP results in increased crystallization temperature and smaller spherulite diameter, due to enhanced nucleation. Incorporation of SiOPh into the polypropylene matrix already modified with the sorbitol does not affect nucleation kinetics of iPP α-spherulites, nor the rate of their growth. Furthermore, transparency is improved on the addition of sorbitol, but somewhat worsened with increasing content of resin. The modified samples are also stiffer, with a decreasing elongation at break and increasing Young's modulus values, with increasing amounts of fillers in the composites. All of the above is attributed to a lack of interaction between iPP, sorbitol derivative and/or siloxane-silsesquioxane resin. Such a result is unexpected, since in principle interactions between the –OH groups present in both modifiers could be predicted. To overcome this problem and favor interactions between the composite components, attempts are made to include compatibilizers in the formulation, as will be detailed in a forthcoming article.

ACKNOWLEDGMENTS

The authors express their great appreciation to Dr. Mariacristina Cocca, Dr. Marilena Pezzuto, Ms. Cristina Del Barone, and Dr. Salvatore Mallardo for their valuable suggestions and help during the development of the research work. Their willingness to give time so generously has been very much appreciated. The authors are also grateful to Milliken & Company for supplying the nucleating agent samples for research. The study was supported by the project "Scholarship support for doctorate students studying at faculties perceived as strategic from Wielkopolska development point of view," submeasure 8.2.2. of Operational Programme "Human Resources Development."

REFERENCES

1. Cocca, M.; Androsch, R.; Righetti, M. C.; Malinconico, M.; Di Lorenzo, M. L. *J. Mol. Struct.* **2014**, *1078*, 114.
2. Lotz, B.; Wittmann, J. C.; Lovinger, A. J. *Polymer* **1996**, *37*, 4979.
3. Turner-Jones, A.; Aizlewood, J. M.; Beckett, D. R. *Makromol. Chem.* **1964**, *75*, 134.
4. Padden, F. J.; Keith, H. D. *J. Appl. Phys.* **1959**, *30*, 1479.
5. Lotz, B. *Macromolecules* **2014**, *47*, 7612.
6. Raab, M.; Scudla, J.; Kolarik, J. *Eur. Polym. J.* **2004**, *40*, 1317.
7. Kristiansen, M.; Werner, M.; Tervoort, T.; Smith, P. *Macromolecules* **2003**, *36*, 5150.
8. Balzano, L.; Rastogi, S.; Gerrit, W.; Peters, M. *Macromolecules* **2008**, *41*, 399.
9. Horvath, Z.; Gyarmati, B.; Menyhard, A.; Doshev, P.; Gahleitner, M.; Varga, J.; Pukanszky, B. *RSC Adv.* **2014**, *17*, 429.
10. Pantani, R.; Coccorullo, I.; Volpe, V.; Titomanlio, G. *Macromolecules* **2010**, *43*, 9030.
11. Fina, A.; Abbenhuis, H. C. L.; Tabuani, D.; Camino, G. *Polym. Degrad. Stab.* **2006**, *91*, 2275.

12. Fina, A.; Tabuani, D.; Frache, A.; Camino, G. *Polymer* **2005**, *46*, 7855.
13. Zhou, Z.; Cui, L.; Zhang, Y.; Zhang, Y.; Yin, N. *J. Polym. Sci. Part B: Polym. Phys.* **2008**, *46*, 1762.
14. Pracella, M.; Chionna, D.; Fina, A.; Tabuani, D.; Frache, A.; Camino, G. *Macromol. Symp.* **2006**, *234*, 59.
15. Wang, X.; Li, J.; Wu, L. *J. Appl. Polym. Sci.* **2011**, *121*, 995.
16. Zhou, Z.; Cui, L.; Zhang, Y.; Zhang, Y.; Yin, N. *Eur. Polym. J.* **2008**, *44*, 3057.
17. Lin, O. H.; Ishak, Z. A. M.; Akil, H. M. *Mater. Des.* **2009**, *30*, 748.
18. Choi, J. H.; Jung, C. H.; Kim, D. K.; Suh, D. H.; Nho, Y. C.; Kang, P. H.; Ganesan, R. *Radiat. Phys. Chem.* **2009**, *78*, 517.
19. Perrin, F. X.; Bruzaud, S.; Grohens, Y. *Appl. Clay. Sci.* **2010**, *49*, 113.
20. Zhao, F.; Bai, X.; McLauchlin, A. R.; Gu, J.; Wan, C.; Kandasubramanian, B. *Appl. Clay. Sci.* **2010**, *47*, 249.
21. Roy, S.; Lee, B. J.; Kakish, Z. M.; Jana, S. C. *Macromolecules* **2012**, *45*, 2420.
22. Roy, S.; Jana, S. C. *Antec. Conf. Proc.* **2011**, *69*, 1.
23. Roy, S.; Scionti, V.; Jana, S. C.; Wesdemiotis, C.; Pischera, A. M.; Espe, M. P. *Macromolecules* **2011**, *44*, 8064.
24. Barczewski, M.; Dobrzyńska-Mizera, M.; Dudziec, B.; Sterzyński, T. *J. Appl. Polym. Sci.* **2014**, *131*, 40131.
25. Di Lorenzo, M. L.; Frigione, M. *J. Polym. Eng.* **1997**, *17*, 429.
26. Hatakeyama, F.; Kanzaki, S. *J. Am. Ceram. Soc.* **1990**, *73*, 2107.
27. Zhang, Y.; Wang, Y.; Hu, A. *RSC Adv.* **2015**, *5*, 70297.
28. Di Lorenzo, M. L.; Cimmino, S.; Silvestre, C. *J. Appl. Polym. Sci.* **2001**, *82*, 358.
29. Vyazovkin, S.; Chrissafis, K.; Di Lorenzo, M. L.; Koga, N.; Pijolat, M.; Roduit, B.; Sbirrazzuoli, N.; Suñol, J. *J. Thermochim. Acta* **2014**, *590*, 1.
30. Norm Tworzywa sztuczne - Oznaczanie współczynnika przepuszczania światła i zamglenia; PN-84/C-89100; **1984**.
31. Romankiewicz, A.; Sterzyński, T.; Brostow, W. *Polym. Int.* **2004**, *53*, 2086.
32. Norm, Plastics—Determination of Tensile Properties—Part 1: General Principles; ISO 527-1:2012; **2012**.
33. Brostow, W.; Hagg Lobland, H. E.; Narkis, M. *J. Mater. Res.* **2006**, *21*, 2422.
34. Brostow, W.; Hagg Lobland, H. E.; Khoja, S. *Mater. Lett.* **2015**, *159*, 478.
35. Szołyga, M.; Dutkiewicz, M.; Marciniec, B.; Maciejewski, H. *Polymer* **2013**, *58*, 766.
36. Launer, P. J.; Arkles, B. Reprinted from Silicon Compounds: Silanes & Silicones, Gelest, Inc Morrisville, PA.
37. Lisovsky, I. P.; Lytovchenko, V. G.; Mazunov, D. O.; Szekeres, A. *Ukr. J. Phys.* **2005**, *50*, 78.
38. Inagaki, S.; Fukushima, Y.; Kuroda, K. *J. Chem. Soc. Chem. Commun.* **1993**, 8, 680.
39. Di Lorenzo, M. L.; Silvestre, C. *Prog. Polym. Sci.* **1999**, *2*, 917.
40. Lopez, L. C.; Wilkens, G. L. *Polymer* **1989**, *30*, 882.
41. Fillon, B.; Thierry, A.; Lotz, B.; Wittmann, J. C. *J. Therm. Anal.* **1994**, *42*, 721.
42. Di Lorenzo, M. L.; Cimmino, S.; Silvestre, C. *Macromolecules* **2000**, *33*, 3828.
43. Smith, T. L.; Masilamani, D.; Bui, L. K.; Khanna, Y. P.; Bray, R. G.; Hammond, W. B.; Curran, S.; Belles, J. J., Jr.; Binder-Castelli, S. *Macromolecules* **1994**, *27*, 3147.
44. Watase, M.; Nakatani, Y.; Itagaki, H. *J. Phys. Chem. B* **1999**, *103*, 2366.
45. Wilder, E. A.; Spontak, R. J.; Hall, C. K. *Mol. Phys.* **2003**, *101*, 3017.
46. Monasse, B.; Haudin, J. M. *Colloid Polym. Sci.* **1985**, *263*, 822.
47. Di Lorenzo, M. L. *Polymer* **2001**, *42*, 9441.
48. Di Lorenzo, M. L. *Prog. Polym. Sci.* **2003**, *28*, 663.
49. Haudin, J. M. In Handbook of Optical studies of polymer morphology; Meeten, G. H. Eds.; Elsevier: Barking, **1986**; p 167.
50. Horvath, Z.; Menyhard, A.; Doshev, P.; Gahleiner, M.; Voros, G.; Varga, J.; Pukanszky, B. *ACS Appl. Mater. Inter.* **2014**, *6*, 7456.
51. Gałęski, A. *Prog. Polym. Sci.* **2003**, *28*, 1643.